Nanoscale strain distribution at the Ag/Ru(0001) interface

H. Zajonz* and Doon Gibbs
Department of Physics, Brookhaven National Laboratory, Upton, New York 11973-5000

A. P. Baddorf and D. M. Zehner
Solid State Division, Oak Ridge National Laboratory, Oak Ridge, Tennessee 37831-6030
(Received 14 November 2002; published 30 April 2003)

We present an x-ray scattering study of the structure and strain distribution of the orthorhombic (20×20) reconstruction of a one monolayer Ag film grown on Ru(0001) at $T=690$ K. The application of very-fast simulated annealing algorithms to the measured x-ray intensities leads to a model in which the Ag film forms a two-dimensionally modulated hexagonal network of dislocations separating smaller patches of ideal hcp and faulted fcc adlayer stacking. Calculations of the in-plane strain distribution based on the model reveal a simple stripelike structure with a 4.5-nm periodicity, reminiscent of what is observed on Cu/Ru(0001).

DOI: 10.1103/PhysRevB.67.155417 PACS number(s): 68.35.Bs, 68.35.Ct, 68.55.−a

INTRODUCTION

There has been increasing interest in recent years in characterizing strain distributions at surfaces and interfaces, particularly within the context of metallic thin film growth. The strain distribution has been identified as one of the key quantities that determines the interfacial structure, and thereby controls the resulting thin film electronic properties. For the bimetallic catalysts composed of Ag or Cu on Ru(0001), for example, it is believed that the catalytic activity may be tuned by varying the interfacial strain,[1–6] which originates in the thin film-substrate lattice mismatch at the interface. A full understanding of these processes has remained elusive, however, in part from the lack of a detailed characterization of the interfacial atomic structure. This problem is particularly challenging in the cases of Ag and Cu films grown on Ru surfaces since they are known to form complex, one and two dimensionally modulated structures, which are ordered on nanometer length scales. On the one hand, scanning probes provide beautiful images, which capture qualitative features of the local structure. On the other hand, diffraction techniques lead to models requiring the determination of many unknown parameters, but this allows the average structure to be obtained over long length scales.

Progress on these problems has recently been made in x-ray diffraction studies of Cu on Ru(0001) through the use of simulated annealing techniques to analyze the measured intensities.[7] In the case of Cu on Ru(0001), the average bulk lattice misfit at the interface is 5.8% leading to a net tensile strain within the Cu film after it is deposited. The resulting bilayer reconstruction has been described by stripes of dislocations in both Cu layers separating regions of faulted fcc and hcp stacking (measured with respect to the Ru substrate). The x-ray scattering studies showed that the stripe periodicity remains commensurate with the substrate, but varies with temperature, taking values between 4 and 5 nm. Such a detailed description of the interfacial structure permitted calculations of the corresponding inplane strain distribution. The strain was likewise found to be inhomogeneous, and ordered in a stripe lattice of nanometer length scale. This leads to a 50% reduction of the average strain relative to a pseudomorphic bilayer.

In this paper we describe the results of x-ray scattering studies of the monolayer reconstruction of Ag on Ru(0001) at $T=690$ K. In contrast to Cu, the bulk near neighbor spacing in Ag is 6.3% larger than that of Ru which leads to an average compressive strain at the interface. Earlier scanning tunneling microscopy (STM) studies have shown that submonolayer Ag forms a two-dimensional dislocation structure on Ru(0001) at room temperature with $a\sim 4\times 6\ \mathrm{nm}^2$ unit cell.[8,9] At higher Ag coverages, a variety of locally ordered (and disordered) structures is observed, including stripelike and herringbone-like structures with long dimensions varying between 6 and 14 nm. After annealing to 800 K and recooling to room temperature, a single Ag monolayer is reported to form a corrugated, herringbone-like structure with $a\sim 5\times 20\ \mathrm{nm}^2$ unit cell.

Here, we report a crystallographic study of the monolayer Ag/Ru(0001) interface in which the film deposition and characterization were carried out at a fixed, high temperature of 690 K. The intensities were fitted to a set of multidimensional modulation functions using simulated annealing techniques. The resulting model of the complex orthorhombic (20×20) reconstruction consists of a distorted, hexagonal dislocation network separating regions of fcc and hcp stackings of the Ag film relative to the underlying Ru(0001) substrate. The average unit cell dimensions are $5.412\times 9.374\ \mathrm{nm}^2$, which are approximately commensurate with the substrate. In addition, it is found that the Ru substrate is laterally undistorted, exhibiting only small relaxations of the interlayer spacing near the interface, and no buckling. On the basis of these results, we have calculated the average in-plane strain distribution across the Ag unit cell at 690 K. Remarkably, it resembles a simple stripe structure with a 4–5-nm stripe separation, similar to what was observed for Cu on Ru(0001). Upon cooling from 690 K to room temperature, our films transform to a more disordered, possibly multiphase structure whose dimensions resemble the submonolayer structure reported earlier on the basis of STM studies.[8,9] Sorting out how the various observed structures

 ©2003 The American Physical Society

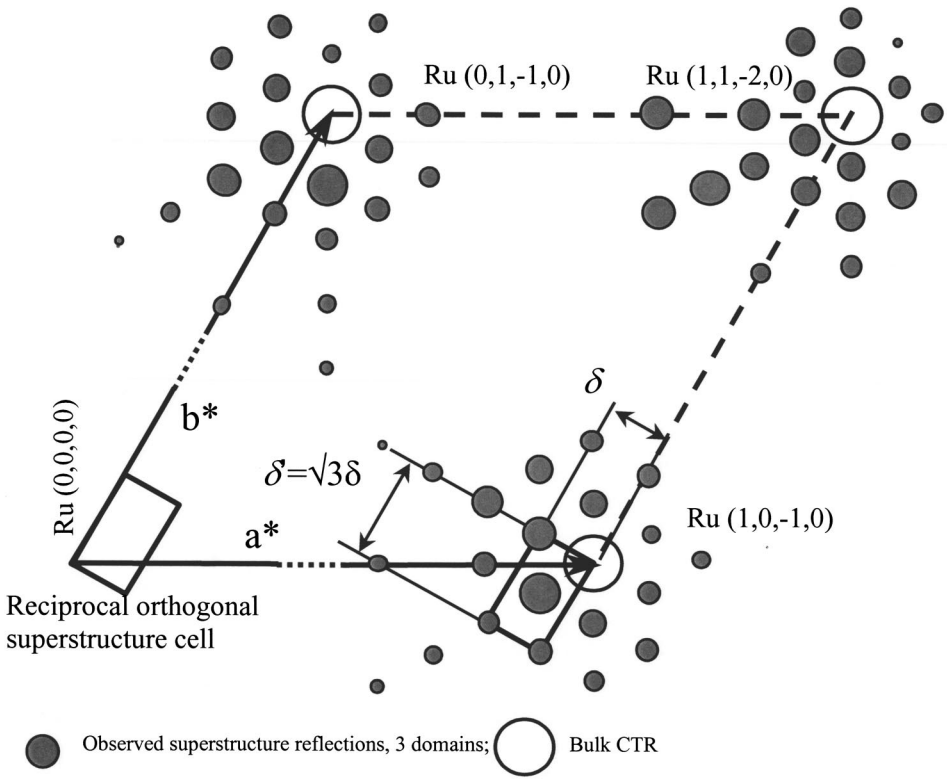

FIG. 1. A section of the in-plane diffraction pattern for Ag on Ru(0001) observed by x-ray scattering.

depend on deposition and annealing history, and exploring the different sensitivities of the two probes to the extent of ordering over a range of length scales, remain fascinating problems for future work. In the following, we describe the experimental procedures used in this work, and then present our results and discussion.

EXPERIMENT

The x-ray scattering experiments reported here were carried out in an ultrahigh vacuum chamber on beamline X22C at the National Synchrotron Light Source. Most details of the experimental setup can be found in Refs. 7 and 10. The Ru crystal had a 10-mm diameter and was polished to within 0.1° of the crystallographic (0001) plane. The bulk mosaic was 0.07° at the (1, 0, −1, 1) reflection. The sample was heated from the back by electron bombardment techniques, and its temperature monitored by a type-*C* thermocouple. After sputtering at 300 K with 1-kV Ar ions followed by repeated oxygen annealing cycles,[10,11] the surface was found to be clean, as determined from Auger electron spectroscopy. With the Ru sample at 690 K, Ag was deposited onto the surface using a resistively heated Knudsen cell. The deposition rate was calibrated from oscillations of the x-ray reflectivity observed at the (0001) position, and set at about 0.1 ML per minute.[12] In all subsequent experiments, the substrate temperature remained fixed at 690 K. This temperature was chosen on the basis of separate studies which showed that the average domain size of the Ag reconstruction reached a maximum of ~800 Å at this temperature.[13] We found, moreover, that the widths of all of the in-plane Ag superstructure reflections broadened substantially upon cooling, corresponding to the reduction of translational order within domains.

A total of 665 integrated in-plane intensities were measured in the *z*-axis geometry at 690 K by rotating the sample around its surface normal and subtracting the diffuse background signal.[14] This set of reflections included symmetry equivalents, which was then reduced to 317 nonequivalent reflections. The error of the diffracted intensities was estimated from the measured reproducibility of symmetry equivalent reflections and produced an internal *R* value of 17% based on $|F|^2$ for all reflections. The data were corrected for the polarization, Lorentz factor, active sample area, and resolution function of the instrument. For the reconstructed surface, we obtained a set of 98 superstructure reflections, including 68 in-plane and 30 rod reflections. In addition, 219 data points from bulk crystal truncation rods CTRs (Ref. 15) were measured along the (0,0,0,L), (1,0,−1,L), (2,0,−2,L), (2,1,−3,L) and (1,1,−2,L) CTRs. Rod data were taken up to a maximum normal momentum transfer of $Q_z = 3.67$ Å^{-1}, which is equivalent to 2.4 reciprocal lattice units. These results are described in the conventional crystallographic notation of the Ru substrate, where at room temperature the in-plane lattice constant $a = 2.706$ Å and, normal to the surface, $c = 4.282$ Å.

RESULTS AND DISCUSSION

Diffraction pattern

A section of the surface diffraction pattern obtained from a close-packed single layer of Ag on Ru(0001) grown at 690 K is shown in Fig. 1. We observe a hexagonal arrange-

ment of superstructure reflections with detectable intensities close to the Ru bulk Bragg reflections, consistent with an orthorhombic (20×20) reconstruction. Each symbol in Fig. 1 indicates a rod oriented parallel to the surface normal direction along which the scattered x-ray intensity is distributed. The large, open circles represent CTRs, which arise from the truncation of the hexagonal Ru substrate. CTR's are indexed using the substrate lattice periodicity and pass through bulk Ru Bragg reflections. The filled circles in Fig. 1 originate from the surface reconstruction, which has a periodicity different from the substrate. The relative sizes of these symbols correspond to the logarithms of the observed (integrated) intensities.

The most intense superstructure reflections observed next to the $(1,0,-1,0)$ Ru CTRs represent the primary Ag peaks. Typical counting rates were 20 000/sec at a 200-mA electron beam current in the storage ring. The absolute value of their wavevectors at 690 K is $|q|=2.2647(2)$ Å^{-1}, which is to be compared with that of the Ru CTR of $|q|=2.3220(2)$ Å^{-1}. Defining a superstructure cell with edges along the [100] and [120] directions, respectively, suggests a two-dimensional reconstruction corresponding to 19×19 Ag atoms lying on top of 20×20 Ru atoms. The smaller satellite reflections near the primary peaks originate from a two-dimensional modulation of the Ag layer, and have intensities up to 1000 times weaker than the primary peaks. Generally, such a modulation results in the loss of site symmetry in three-dimensional space, and leads in this case to an orthorhombic superstructure cell of average dimensions $5.412\times9.37\,(\mathrm{nm})^2$. The width of the primary satellites at 690 K was measured along the (010) direction and found to be $\sim$0.001 rlu, which corresponds to an in-plane correlation length of about 800 Å.

The separations between the primary and higher order peaks give the incommensurabilities δ and δ' of the system, and define a two-dimensional reciprocal space unit cell (shown by the rectangle in Fig. 1). The average periodicity along **a** is increased by a factor of $1/\delta$ with $\delta\sim1/20$. The real space superstructure lattice vector **b** is enlarged by a factor of $1/\delta'$ (with $\delta'\sim\sqrt{3\delta}$) and rotated by $\sim30°$ with respect to the corresponding hexagonal lattice vector of the Ru(0001) substrate. It is interesting that during deposition the value of the primary Ag wave vector shifts abruptly at monolayer completion toward the commensurate value $\delta=1/20$. This is reminiscent of the lock-in behavior observed upon completion of a Cu bilayer on Ru(0001).[10] However, in the present case the values of δ and δ' continue to increase slightly with increasing coverage above 1 ML (by $\sim$0.001 Å^{-1}/5 ML), and we defer a discussion of the possible commensurability to a later paper.[10]

The x-ray diffraction pattern obtained at 690 K differs from the idealized patterns that might be expected on the basis of the structures reported in the STM studies.[8,9] For example, the pattern expected for an ordered herringbone-like structure is comprised of two independent length scales, the first arising from the underlying stripe periodicity, and the second corresponding to the elbow or kink periodicity.[16] These are not observed at high temperature. We suspect that the origin of these differences lies in the sample preparation procedures. The monolayer films in the STM study were grown at room temperature, flash annealed to 800 K, and then cooled to 300 K. In contrast, our films were grown and studied at elevated substrate temperatures (690 K), which we believe favors equilibrium film growth, consistent with our observation of the largest ordered domains at higher temperatures. However, even when grown at elevated temperatures, the Ag monolayer does not exhibit true long-range order, which would correspond to resolution-limited peak widths, nor are we able to prove that the present growth conditions correspond to equilibrium. These kinds of issues have also been encountered with the Cu/Ru(0001) system in which differences among the structures reported by STM and x-ray diffraction[10] also appear to depend on annealing history.

It is important to note in the present case that upon cooling from 690 K to room temperature, the x-ray diffraction peaks observed from the Ag monolayer broaden, and at 570 K the film transforms to a new, more disordered structure. This is illustrated in Fig. 2(c), which shows mesh plots of the logarithm of the measured intensities around the Ru$(1,0,-1,0.15)$ CTR at 420 and 590 K (left and right, respectively). In order to display the hexagonal pattern of the Ag superstructure reflections in an orthogonal coordinate system their coordinates have been transformed as $H_{\mathrm{rec}}=H_{\mathrm{hex}}$ and $K_{\mathrm{rec}}=H_{\mathrm{hex}}+2*K_{\mathrm{hex}}$. At 420 K, there is an increase of the unit vector $\mathbf{a}'$ by a factor of 1.5 along all of the close-packed directions. This corresponds to unit cell dimensions of $\sim5\times6\,\mathrm{nm}^2$ which is close to those reported by STM for submonolayer Ag coverages at room temperature. There is, in addition, a considerable broadening of all peaks, and a band of diffuse scattering which connects the primary Ag harmonics of the high-temperature structure. A typical primary peak width in the lower temperature phase measured along the $[0,1,0]_{\mathrm{rec}}$ direction is 0.0126 Å, which is 50% broader than the peak width at 590 K [see Fig. 2(b)]. These correspond to correlation lengths of 500 and 800 Å respectively (calculated as 2π/full width at half maximum). Unfortunately, it is very difficult to make quantitative statements about such a disordered structure, and we have not pursued the analysis further in this paper. However, it seems possible that some or all of the local structures observed in the STM studies may be represented in the lower temperature diffraction pattern with limited correlation lengths.

Data and parameters

In order to obtain a model for the reconstructed Ag surface at 690 K calculations were carried out using all 98 independent superstructure reflections and 219 CTR reflections simultaneously. Since the CTR data represent a coherent superposition of bulk and superstructure scattering, they introduce a phase contrast, which can strongly influence the scattered intensities between Bragg reflections. This further constrains models of the structure and orientation of the adlayer with respect to the substrate unit cell. In contrast, the superstructure data originate only from the Ag monolayer reconstruction. However, fitting the superstructure and CTR

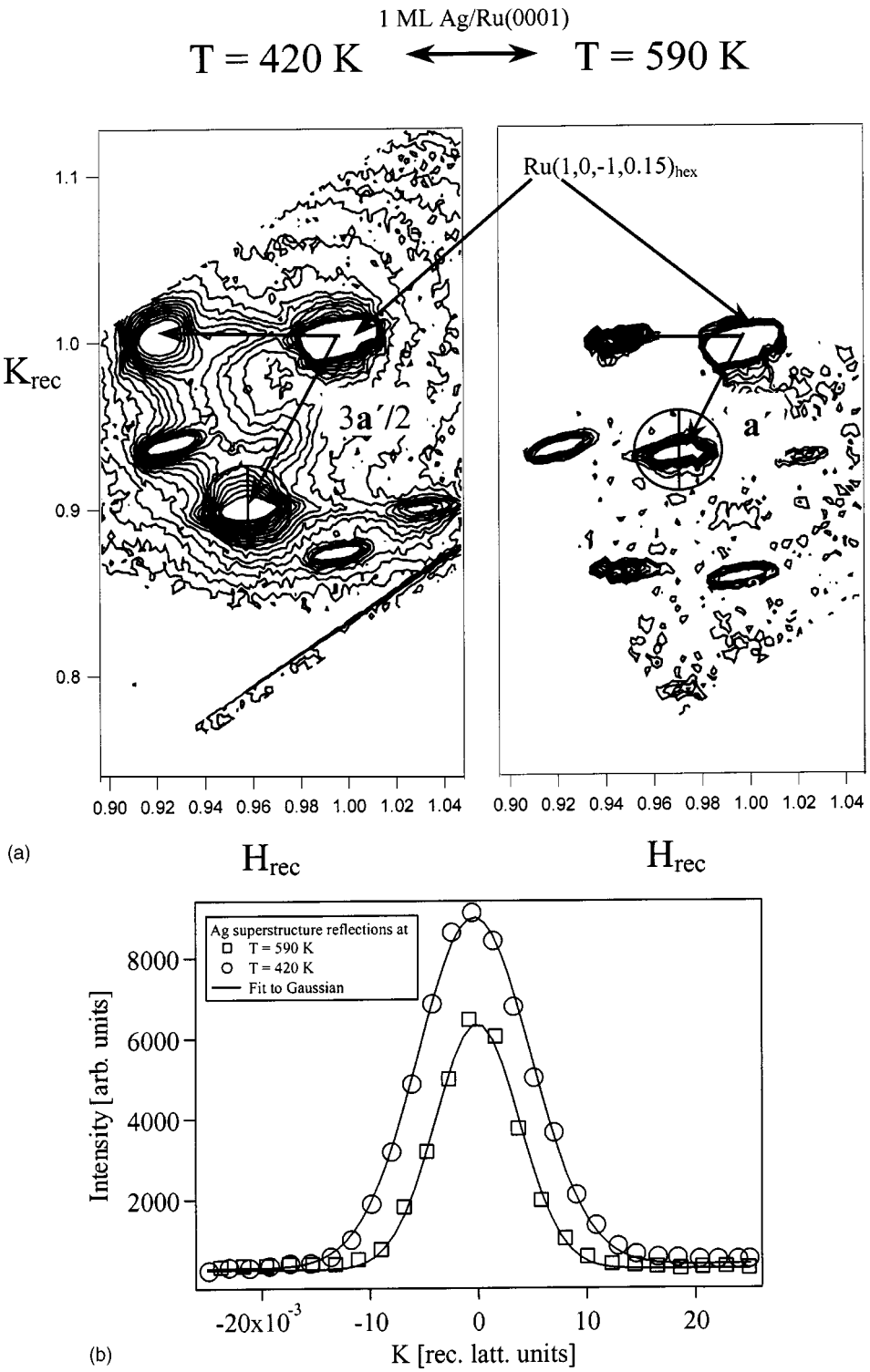

FIG. 2. (a) Contour plots of the observed x-ray intensities around the Ru (1,0,−1,0.15) reflection at 420 K (left) and 590 K (right). (b) Scans of the primary Ag satellite along the [010] direction at 590 K (circles) and 420 K (squares).

data together permits finer distinctions to be made among different models and enhances the overall reliability of the analysis.

Due to the presence of steps (and the phase symmetry of the Ru(0001) substrate) the surface exhibits a maximum of six rotational domains, which requires an incoherent intensity averaging of overlapping CTR and superstructure rod intensities. The model parameters include 20 coefficients to describe the modulation of the Ag layer, three (topmost) layer distances, two scaling factors (for in-plane and out-of-plane data), and a roughness parameter β.[15] This corresponds to 26 parameters in all. The parameters were determined using an adapted fast-simulated, reannealing algorithm[17,18] that was implemented in a program which is able to describe a wide variety of modulated surface configurations. To avoid the dominance of strong CTR reflections during the refinement, we minimized a weighted residual with respect to the logarithm of the measured intensity.[19] Our best fit resulted in

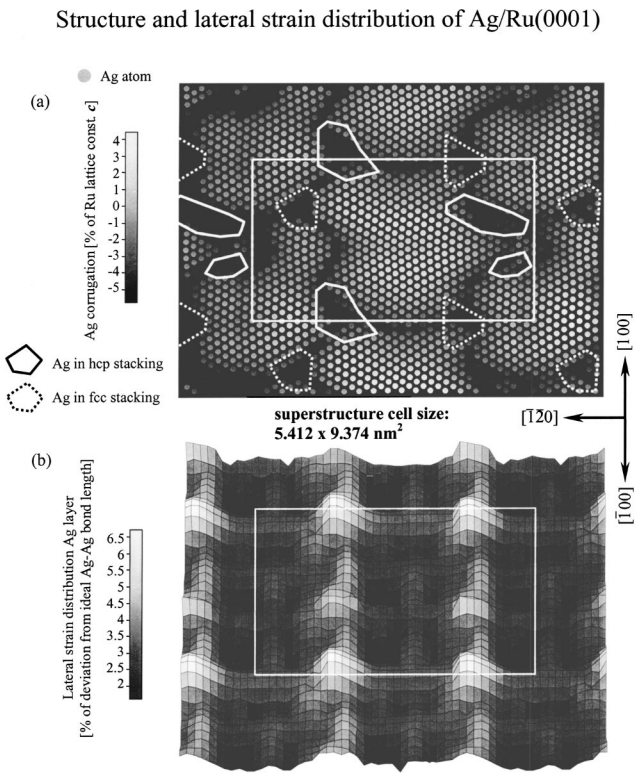

FIG. 3. (a) Top view of the orthorhombic (20×20) reconstruction of Ag/Ru(0001). The Ru substrate is not shown. The shading indicates the extent of corrugation. (b) Lateral strain distribution as a function of atom position. The shading indicates the percent deviation from bulk Ag-Ag spacing.

$R_w(\log_{10}[l])=5.5\%$ for a model with $P1$ symmetry. It should be noted in this respect that other adlayer symmetries (including $P6$, $P3$, and $P2$) were also considered, but these always gave weighted residuals greater than 20%. It is worth adding that the use of modulation functions in the fitting instead of the displacements of independent atoms within the unit cell implies that the number of free parameters in the model depends not on its symmetry, but rather on the number of Fourier components employed.

Model and method

Figure 3 shows an on-top view of the model, which was derived from our x-ray diffraction data. The circles represent the Ag atoms. The degree of shading is proportional to the corrugation on the Ru substrate, which depends mainly on the adsorption site. Possible adsorption sites range from hollow to bridge to on-top sites, in addition to the dislocation sites between these. Our analysis suggests that the substrate does not laterally reconstruct and it is, therefore, not displayed in Fig. 3. However, vertical relaxations of the top three interlayer spacings (including the Ag layer) were necessary to obtain a good fit of the out-of-plane data, as will be shown later.

The average Ag reconstruction is dominated by a large, hexagonally distorted, two-dimensional dislocation network reminiscent of the misfit dislocation structure observed by Hwang *et al.*[8] in an earlier STM study at submonolayer coverage. Our analysis shows further that the dislocation regions are separated by small regions of fcc and hcp stacking of the top layer with the Ru substrate, which is also hexagonal. The small hcp and fcc regions in the Ag film are indicated by polygons in the superstructure cell with solid and dashed lines, respectively. Within these polygons, the Ag atoms experience an optimized Ag/Ru coordination, together with a significant compressive strain relative to Ag bulk. The dimensions of these highly strained regions within the unit cell are relatively small in comparison to the dislocation arrays, which accounts for the net strain relaxation at the surface. It also appears plausible that the network of hcp and fcc patches with maximum coordination at the interface play a role in driving the wave vector of the reconstruction toward the commensurate value of 1/20 under the given conditions. From this perspective, the reconstruction may be viewed as an hexagonal array of dislocation domains, separated by patches of hcp and fcc stacking. In this sense, it is a disordered two-dimensional analog of the uniaxial stripe-phase reconstruction, which occurs for bilayer films of Cu on Ru(0001).

The details of the lateral Ag reconstruction are described by a set of two dimensional modulation functions. A set of periodic functions, which proved to be suitable for the present problem, is

$$f_x(x,y)=a_{1,1}\sin(2\pi x+p_{1,1})+a_{1,2}\sin(3\pi x+p_{1,2})+a_{1,3}\sin[4\pi x+p_{1,3}]+a_{1,4}[1-\cos(2\pi y+p_{1,4})]+a_{1,5}[1-\cos(4\pi y+p_{1,5})], \tag{1a}$$

$$f_y(x,y)=a_{2,1}\sin(2\pi x+p_{2,1})+a_{2,2}\sin(3\pi\cdot x+p_{2,2})+a_{2,3}\sin(4\pi\cdot x+p_{2,3})+a_{2,4}[1-\cos(2\pi y+p_{2,4})]+a_{2,5}[1-\cos(4\pi y+p_{2,5})], \tag{1b}$$

These functions are combined Fourier series in which the arguments depend on the position components x and y of the Ag atoms within the superstructure cell. The partial series that is dependent on x or y can be truncated after the second or third term depending on the quality of the fit. Equation (1a) represents a periodically modulated transverse displacement of Ag atoms along the [100] direction, which is coupled to a modulated longitudinal displacement of Ag chains along [120]. Equation (1b) is analogous to Eq. (1a) except that the displacements are rotated by 90° with respect to those in Eq. (1a). This form permits a wide variety of modulated configurations to be examined. The final model is derived by adding the value of the specific modulation function $f_x(x,y)$ and $f_y(x,y)$ to the x or y component of each atom of the unmodulated arrangement. The argument x or y in $f(x,y)$ defines the

atom position along the inplane superlattice vector **a** or **b**, respectively.

The matrices $\mathbf{A}=\begin{pmatrix} a_{11} & a_{12} & a_{13} & a_{14} & a_{15} \\ a_{21} & a_{22} & a_{23} & a_{24} & a_{25} \end{pmatrix}$ and $\mathbf{P}=\begin{pmatrix} p_{11} & p_{12} & p_{13} & p_{14} & p_{15} \\ p_{21} & p_{22} & p_{23} & p_{24} & p_{25} \end{pmatrix}$ contain the amplitudes and phases of the Fourier components, respectively. They represent the parameters which ultimately determine the 1444 x and y components of the laterally modulated structure of the Ag film. $f_x(x,y)$ and $f_y(x,y)$ are then incorporated into the phase factor of the superstructure amplitude, which models the diffracted intensity as follows:

$$l_{\mathrm{surf}}(hkl) = S\left|\sum_n f_n(hkl)e^{2\pi i\{h[x_n+f_x(x_n,y_n)]+k[y_n+f_y(x_n,y_n)]+lz_n\}}\right|^2. \tag{2}$$

The indices h, k, and l are the components of the reciprocal lattice vector of a specific reflection. $f_n(hkl)$ is the form factor, which describes the scattering of the nth atom with respect to a particular wavevector. (x_n,y_n,z_n) are the coordinates of the nth atom relative to the unmodulated layer. The parameter S is a scale factor, which contains model independent constants. The surface roughness was modeled in the Gaussian approximation by an additional factor R_β, which multiplies the square of the structure factor for the CTR intensities.[15] R_β has the general form $(1-\beta)^2/(1+\beta^2-2\beta\cos 2\pi|)$ where $\beta(0<\beta<1)$ reflects the fractional occupancy of atoms in the surface layer as a result of steps. Complete expressions for the surface and CTR intensities have been published elsewhere and will not be repeated here.[7,12]

Due both to the complexity of the nonlinear function to be fitted, and to significant correlations among the model parameters, least squares fitting methods are not well suited to this problem. Therefore, we used very fast-simulated, reannealing algorithms[17,18,20] to determine the matrices **A** and **P**, the surface roughness S and the interlayer distances. Simulated annealing is in principle capable of finding the best global fit to a nonlinear function in a multidimensional parameter space. Its primary advantage is its ability to move away from the local optima of the cost function, which needs to be minimized. Thus, in comparison to least square refinement techniques, its ability to find the global optimum is not confined to the initial conditions, which are given by the start model. It is, nevertheless, a prerequisite that the theoretical model must be able to describe the actual atomic arrangement accurately, and the diffraction data must be sensitive to a particular model. Here the in-plane data set turned out to be very sensitive to the lateral arrangement of the Ag atoms on the Ru(0001) surface. The computing time required to examine 30 000 models with six domains of 2326 atoms per unit cell (and for 317 reflections) was 36 h using a Pentium III 500-MHZ processor.[21]

Results

The matrices **A** and **P** in Eqs. (1a) and (1b) were determined as

	a_{i1}	a_{i2}	a_{i3}	a_{i4}	a_{i5}
$f_x(x,y), i=1$	0.0080	0.0025	0.0000	0.0020	−0.0038
$f_x(x,y), i=2$	0.0045	−0.0019	−0.0031	0.0019	−0.0030
	p_{i1}	p_{i2}	p_{i3}	p_{i4}	p_{i5}
$f_x(x,y), i=1$	16.9	−81.6	1.67	20.8	139.3
$f_y(x,y), i=2$	−10.9	0.97	1.00	−10.7	7.51

The roughness parameter β was found to be 0.23(4), a value that is reasonable for metal surfaces as defined by Robinson.[15] From this we may calculate a root mean squared deviation of the height-height correlation function, $\sigma_{\mathrm{RMS}}=d_{\mathrm{Ru}}\sqrt{\beta}/(1-\beta)$. Its value is 1.3 Å,[12] which is close to the single step height $d_{\mathrm{Ru}}=c/2$ of the Ru substrate. Our treatment did not include a domain size distribution, which is equivalent to assuming that the steps are uncorrelated.

The best fit to all of the measured data is shown in Figs. 4(a)–4(c). Figure 4(a) compares the calculated intensities of the $(hk0)$ satellite reflections to the measured intensities on a log-log scale. These intensities are most sensitive to the in-plane surface structure and play a central role in its determination. If the model were in perfect agreement with the experiment, all of the data points would fall on the solid line. As may be seen, the agreement is excellent.

Interlayer relaxations among the Ag layer and the subsequent two Ru layer spacings were also considered in our calculations. However, relaxations between deeper layers did not improve the fitting and they were assumed to adopt the bulk Ru interlayer spacing. Our fits of the out-of-plane data including the reflectivity, off-specular, and superstructure data are displayed in Figs. 4(b) and 4(c). The solid lines represent the model, and the diamonds the experimental data. We found that a simple hard sphere model of the Ag corrugation measured with respect to the Ru substrate gave the best fit of the out-of-plane structure (see Fig. 5), in contrast to the significant buckling proposed for the interface at room temperature on the basis of STM studies.[8] The average spacing determined between the corrugated Ag layer and the Ru substrate (d_{12}) indicates a constant 3.60(6)% contraction with respect to the $c/2$ lattice constant of Ru. The contraction between the top Ru layer and the subsequent Ru layer, d_{23}, was 0.50(4)%. d_{34} is only slightly compressed by 0.18(6)%.

Strain accommodation

The formation of nanometer length scale dislocation arrays enables lateral strain accommodation through the adjustment of near neighbor distances among Ag atoms. This reduces the average density of the Ag layer with respect to the underlying Ru substrate and provides a more bulk-Ag-like lattice spacing. This phenomenon has also been observed at the Cu/Ru(0001) interface[10,22,23] and on clean Au(111) (Ref. 16) and Pt(111) (Ref. 24) surfaces. At the Cu/Ru(0001) interface[10,22,23] a tensile strain originating in the 5.8% film/substrate lattice mismatch leads to the formation of uniaxial dislocation arrays separating regions of hcp and fcc stacking

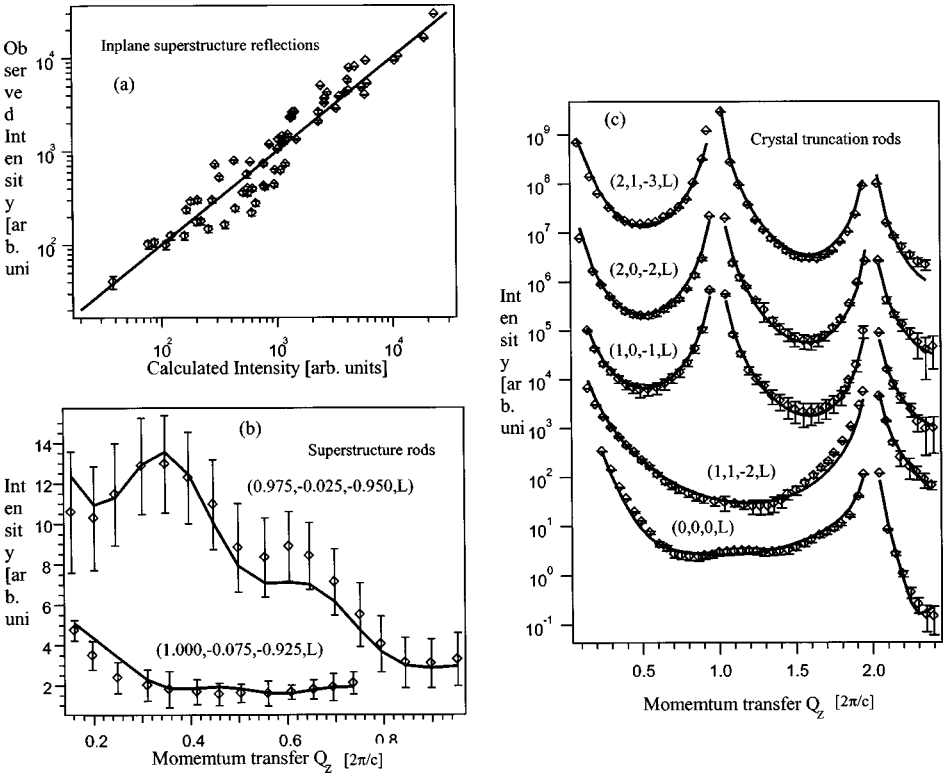

FIG. 4. (a) In-plane ($HK0$) superstructure intensities plotted as a function of their calculated values on a log-log scale. (b) Plot of the intensity of two superstructure rods as function of momentum transfer perpendicular to the surface. The diamond symbols are the experimental values; the solid line represents the best fit based on the model shown in Fig. 2(a). (c) Intensity distribution along different crystal truncation rods plotted vs momentum transfer.

(stripes). Typical stripe-phase separations vary between ~4 and 5 nm depending on temperature.[10] In that case, the existence of a uniaxial reconstruction suggests that the strain relief occurs preferentially in one of the close-packed directions within a domain. Perpendicular to that direction, the adlayer remains pseudomorphic with the substrate and experiences significant tensile strain.[25] This behavior appears consistent with a balance of the strain, on the one hand, and the strong chemical affinity between adlayer and substrate on the other hand.

Interestingly, the adlayer coupling seems to be less important in the Ag/Ru system, a point that is supported by the fact that a simple hard sphere model describes the Ag corrugation. In addition, we found no evidence for pseudomorphic stacking in any direction of the Ag film, although nearly commensurate wave vectors still describe the Ag unit cell dimensions at high temperatures. Instead of one-dimensional (1D) stripes of hcp and fcc phases, we observe a 2D hexagonal-like arrangement of dislocation domains separated by smaller patches of hcp and fcc stacking. As a rough comparison, the average ratio of the areas supporting dislocations to those exhibiting hcp or fcc stacking is greater by a factor of 4 for Ag/Ru(0001) than for Cu/Ru(0001).

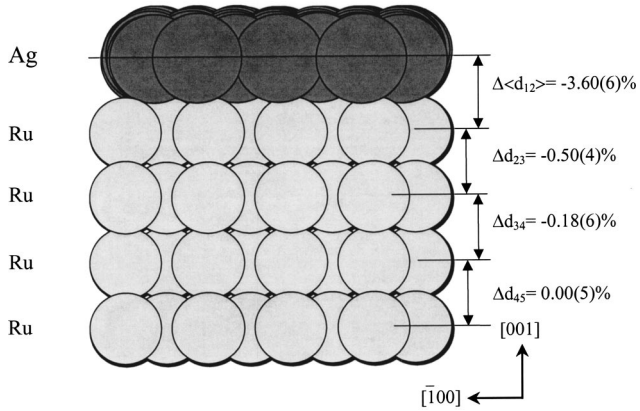

FIG. 5. Simple hard sphere model showing a side view of the observed Ag/Ru(0001) reconstruction. The average interlayer relaxations are indicated on the right hand side with reference to $C_{Ru}/2$ (2.1407 Å).

A detailed characterization of the average surface structure allows the calculation of the lateral residual strain in the Ag layer in terms of the deviations from the bulk Ag-Ag bond lengths. The strain is defined here as the average deviation of the Ag-Ag bond lengths from the six nearest neighbors around each Ag atom. Figure 3(b) shows the lateral strain distribution of the reconstructed Ag film as a function of atom position for the model shown in Fig. 3(a). It turns out that the average strain/atom is reduced to about 3%, compared with the theoretical lattice misfit of 6.3%. The remaining strain distribution, however, is highly inhomogeneous. It peaks in an orthogonal network of ridges with maximum bond length deviations of up to 7%. The regions of elevated compressive strain shown in Fig. 3(b) occur in and around the hcp and fcc patches in the film. Strain accommodation occurs mainly in the regions of large misfit dislocation. The Ag-Ag bond lengths in these regions show only 1–3 % deviations from their bulk values. Thus, although the atomic structure is complex, the underlying strain distribution has an approximately stripelike structure with a stripe separation of about $4\frac{1}{2}$ nm, which is qualitatively similar to what has been observed for the bilayer reconstruction of Cu/Ru(0001).[7,24] This result simply reflects the fact that the hcp and fcc patches in the Ag/Ru reconstruction tend to align

within the unit cell. In contrast, for Cu/Ru(0001) [as well as for Au and Pt (111)] the hcp and fcc domains themselves comprise the stripes. The similarities among the nanometer strain lattices in all these cases points to the importance of long wavelength elastic interactions of the film with the substrate, but a detailed understanding is still lacking.

An interesting final point concerns unpublished calculations of Thayer and Bartelt,[26] who find that our proposed model is not an energy minimum of the Frenkel-Kontorova model. In their simulations, they find that our structure instead relaxes to a ''bright star'' structure. When we calculate the corresponding diffraction intensities, however, we find that they are in clear quantitative disagreement with the measured data. This discrepancy remains unresolved.

We conclude by noting that the structural properties of Ag/Ru(0001) appear highly history dependent. We stress in this regard that the structures whose crystalline perfection most approaches true long range order are those grown (and characterized) at elevated temperatures, which we interpret as closest to equilibrium. The eventual use of systems such as Ag or Cu on Ru(0001) in real applications, whether as bimetallic catalysts or as templates for nanoassemblies, will ultimately depend on our ability to fabricate reproducible, long-range ordered structures. For this reason, we believe that sorting through the complexities of the structures observed by scanning probe and diffraction techniques and understanding their connection to sample history is important.

SUMMARY

We have described an x-ray diffraction study of the structure of a single-layer Ag film on Ru(0001) at 690 K. The structure was solved using very fast-simulated reannealing techniques. We found that the orthorhombic (20×20) reconstruction consists of a single Ag layer with an extended two-dimensional dislocation pattern, separating smaller patches of fcc and hcp stacking from regions supporting dislocations. The details of the in-plane structure are described by a set of two-dimensional modulation functions that can be used to calculate the strain distribution on an atomic level. Through the reconstruction, the theoretical lattice misfit of -6.3% is reduced to an average value of -3%. The calculated strain distribution is highly inhomogeneous and peaks in an orthogonal network of ridges of strain with a 4–5-nm separation. The result is strikingly similar to what is observed in the reconstruction of a bilayer of Cu on Ru(0001). The analysis of the out-of-plane data suggests that the corrugation of the Ag layer follows a hard sphere model. The average interlayer spacing measured with respect to the underlying Ru substrate is compressed by 3.6%. We found no indication that the Ru layers reconstruct laterally, however, the first two Ru interlayer distances are slightly compressed.

ACKNOWLEDGMENTS

We appreciate the help of our colleagues Scott Coburn, Norm Bartelt, Juan De La Figuera-Bayon, John Hamilton, Bob Hwang, Karsten Pohl, Andreas Schmidt, and Gayle Thayer. Work performed at Brookhaven was supported by the U.S. DOE, under Contract No. DE-AC02-98CH10886. Research at Oak Ridge National Laboratory was sponsored by the U.S. DOE under Contract No. DE-AC05-00OR22725 and managed by UT-Battelle, LLC.

*Now at the MPI Für Metallforschung, 70569 Stuttgart, Germany.

[1] J. H. Sinfelt, *Bimetallic Catalysts* (Wiley, New York, 1983).
[2] C. H. F. Peden and D. W. Goodman, J. Catal. **104**, 347 (1987).
[3] J. A. Rodriquez and D. W. Goodman, Surf. Sci. Rep. **14**, 1 (1991).
[4] J. C. Osborne, J. Appl. Phys. **53**, 1586 (1982).
[5] M. Mavrikakis, B. Hammer, and J. K. Nørskov, Phys. Rev. Lett. **81**, 2819 (1998).
[6] M. Gsell, P. Jakob, and D. Menzel, Science **280**, 717 (1998).
[7] H. Zajonz, Doon Gibbs, A. P. Baddorf, and D. M. Zehner, Phys. Rev. B **62**, 10 436 (2000).
[8] R. Q. Hwang, J. C. Hamilton, J. L. Stevens, and S. M. Foiles, Phys. Rev. Lett. **75**, 4242 (1995).
[9] J. L. Stevens and R. Q. Hwang, Phys. Rev. Lett. **74**, 2078 (1994).
[10] H. Zajonz, Doon Gibbs, A. P. Baddorf, and D. M. Zehner, Surf. Sci. Lett. **447**, L141 (2000).
[11] A. P. Baddorf, H. Zajonz, D. Gibbs, and D. M. Zehner (unpublished).
[12] H. Zajonz, D. Gibbs, A. P. Baddorf, and D. M. Zehner, in *Exploration of Subsurface Phenonema by Particle Scattering*, edited by N. Lam, S. Sinha, and C. A. Melendres (IASI Press, New York, 2000), p. 149.
[13] H. Zajonz, A. P. Baddorf, Doon Gibbs, and D. M. Zehner (unpublished).
[14] I. K. Robinson, in *Handbook of Synchrotron Radiation*, edited by E. O. Moncton and G. S. Brown (North Holland, Amsterdam, 1990), Vol. 3.
[15] I. K. Robinson, Phys. Rev. B **33**, 3830 (1986).
[16] A. R. Sandy, S. G. J. Mochrie, D. M. Zehner, K. G. Huang, and Doon Gibbs, Phys. Rev. B **43**, 4667 (1991).
[17] A. L. Ingber, J. Mathl. Comput. Modelling **12**, 967 (1989).
[18] A. L. Ingber, Phys. Rev. A **42**, 7057 (1990).
[19] $R_w\,[\log[I]] = \Sigma_{hkl}|\log_{10}[|F_{hkl}^{\mathrm{OBS}}|^2] - \log_{10}[|F_{hkl}^{\mathrm{CALC}}|^2]|/\Sigma_{hkl}\log_{10}[|F_{hkl}^{\mathrm{OBS}}|^2]$, where $|F_{hkl}^{\mathrm{OBS}}|^2$ is the measured intensity and $|F_{hkl}^{\mathrm{CALC}}|^2$ the calculated intensity.
[20] N. Metropolis, A. W. Rosenbluth, M. N. Rosenbluth, A. H. Teller, and E. Teller, J. Chem. Phys. **21**, 1087 (1953).
[21] Code was compiled with a Microsoft Visual C++ compiler, version 6.0 (1998).
[22] C. Günther, J. Vrijmoeth, R. Q. Hwang, and R. J. Behm, Phys. Rev. Lett. **74**, 754 (1995).
[23] Ch. Ammer, K. Meinel, H. Wolter, A. Beckmann, and H. Neddermeyer, Surf. Sci. **375**, 302 (1997).
[24] G. Grübel, K. G. Huang, D. Gibbs, D. M. Zehner, A. R. Sandy, and S. G. J. Mochrie, Phys. Rev. B **48**, 18 119 (1993).
[25] This domain anisotropy is balanced over macroscopic length scales by the occurrence of stripe domains associated with all three in-plane symmetry directions.
[26] G. Thayer and N. Bartelt (private communication).